Poultry Science

Citrus pectin modulates chicken peripheral blood mononuclear cell proteome in vitro

G. Ávila [*], M. Bonnet [†], D. Viala,[†,‡] S. Dejean [§], G. Grilli [*], C. Lecchi,[*] and F. Ceciliani [*,1]

[*]*Department of Veterinary and Animal Sciences, Università Degli Studi di Milano, 26900, Lodi, Italy;* [†]*INRAE, Université Clermont Auvergne, Vetagro Sup, UMR Herbivores, 63122, Saint-Genès-Champanelle, France;* [‡]*INRAE, Metabolomic and Proteomic Exploration Facility, Proteomic Component (PFEMcp), F-63122 Saint-Genès-Champanelle, France; and* [§]*Institut de Mathématiques de Toulouse, Université de Toulouse, CNRS, UPS, 31062 Toulouse, France*

ABSTRACT Citrus pectin (**CP**) is a dietary fiber used in animal nutrition with anti-inflammatory properties. CP downregulates chicken immunoregulatory monocytes' functions, like chemotaxis and phagocytosis, *in vitro*. The molecular underlying background is still unknown. This study investigated the activity of CP on chicken peripheral blood mononuclear cells (**PBMC**) proteome. An overall number of 1503 proteins were identified and quantified. The supervised sparse variant partial least squares—discriminant analysis (sPLS-DA) for paired data highlighted 373 discriminant proteins between CP-treated and the control group, of which 50 proteins with the highest abundance in CP and 137 in the control group were selected for Gene Ontology (**GO**) analyses using ProteINSIDE. Discriminant Protein highly abundant in CP-treated cells were involved in actin cytoskeleton organization and negative regulation of cell migration.

Interestingly, MARCKSL1, a chemotaxis inhibitor, was upregulated in CP-treated cells. On the contrary, CP incubation downregulated MARCKS, LGALS3, and LGALS8, which are involved in cytoskeleton rearrangements, cell migration, and phagocytosis. In conclusion, these results provide a proteomics background to the anti-inflammatory activity of CP, demonstrating that the *in vitro* downregulation of phagocytosis and chemotaxis is related to changes in proteins related to the cytoskeleton.

Key words: citrus pectin, chicken PBMC proteome, anti-inflammatory, cell migration

2024 Poultry Science 103:104293
https://doi.org/10.1016/j.psj.2024.104293

INTRODUCTION

Pectins are complex polysaccharides present in all plants' cell walls but primarily abundant in citrus fruits (Sahasrabudhe et al., 2018) and made of repeating galacturonic acid units linked by glycosidic linkages (Ridley et al., 2001). Citrus pectin (**CP**) is widely used as dietary fiber with beneficial immunomodulatory and anti-inflammatory effects (Salman et al., 2008; Sahasrabudhe et al., 2018; Beukema et al., 2020) in both human and animal nutrition (Langhout and Schutte, 1996; Leclere et al., 2013). CP inhibits the *in vitro* production of proinflammatory cytokines (IL-1β) and upregulates anti-inflammatory cytokines (IL-1ra and IL-10) in human peripheral blood mononuclear cells (**PBMC**) (Salman et al., 2008). CP also inhibits Toll-like receptors 1 and 2 (TLR1 and TLR2) proinflammatory pathways in human macrophages by blocking TLR2 and potentially reducing NFκB activation, downregulating proinflammatory cytokines and galectin-3 (Sahasrabudhe et al., 2018; Beukema et al., 2020). Although citrus pectin is used as a feed additive in poultry nutrition, its molecular effect on the immune system has been poorly investigated. The peel from *Citrus sinensis* (a source rich in pectin) has been demonstrated to decrease the growth of potential pathogens Staphylococcus aureus, Bacillus cereus, Listeria monocytogenes and yeasts, and molds (Pourhossein et al., 2015). A recent study in broiler quails demonstrated that methanolic extracts of Citrus peeling increased several parameters, including feed intake, weight gain, Feed Conversion Rate, and digestibility coefficient (Ahmad et al., 2024). In broilers, due to the molecular structure of the pectin, pectin levels in feed affect intestinal transit time, feed digestibility, and intestinal viscosity. Therefore, CP supplementation improves energy utilization and nutrient digestibility, increasing productive performance (Silva et al., 2013).

Received June 23, 2024.
Accepted August 29, 2024.

[1]Corresponding author: fabrizio.ceciliani@unimi.it

In a model of chicken coccidiosis, CP had a beneficial effect, decreasing the number of schizonts in the ileal enterocytes by decreasing the serosa thickness. Further effects include an anti-inflammatory activity in the cytokine network by down-regulating the abundance of pro-inflammatory cytokine IL-12β and upregulating pro-inflammatory cytokines, like INFγ and IL-1β (Wils-Plotz et al., 2013). *In vitro* studies on CACO-2 cells demonstrated that CP decreases IL-8 abundance and pathogen adhesion and invasion while increasing probiotic adhesion (de Paula Menezes Barbosa et al., 2020). These results must be validated in chicken. The role of CP in animals has been recently reviewed (Sundaram et al., 2022).

We have previously provided evidence of CP anti-inflammatory activity on monocytes by suppressing their chemotaxis and phagocytosis *in vitro* (Ávila et al., 2021). However, the molecular mechanisms behind these anti-inflammatory effects remain elusive, and no studies on CP's molecular impact on chicken mononuclear cells are available.

Proteomics analysis is the large-scale analysis of the protein profile in biological systems: it has been applied to animal science, allowing a better comprehension of both physiological and pathological events (Almeida et al., 2021). Limited studies on chicken PBMC proteomics are available, primarily on infectious diseases (Korte et al., 2013; Deng et al., 2014; Sekelova et al., 2017) or specific immunological pathways (Deeg et al., 2020). The present investigation aims to increase the knowledge about the positive effects of CP in poultry by assessing the molecular background of the immunomodulatory activity of CP's toward chicken PBMC by determining the untargeted proteome using nano-LC-MS/MS spectrometry.

MATERIALS AND METHODS

Purification of Chicken PBMC From Blood

As previously described, chicken PBMCs were isolated from peripheral blood through double discontinuous gradient centrifugation (Ávila et al., 2021). Briefly, 50 mL of pooled blood from several chickens were used for each experiment. Each experiment was replicated with 7 different peripheral blood pools (biological replicates) from 42-day-old hybrid healthy broilers (ROSS 308) collected during routine slaughtering procedures at a local slaughterhouse in sterile flasks containing 0.2% EDTA. The blood was collected in the sterile flasks by gravity during the exsanguination procedure. The flasks were immediately put at 4° degrees in a cooler, and the purification procedure started within 1 h of the blood collection. The purification procedure began by mixing the blood with 1% methylcellulose (GE Healthcare, Bio-Sciences AB, Uppsala, Sweden) and centrifuging at 40 x g without brakes for 30 min at 4°C. Then, the supernatant diluted (1:1) with sterile PBS without Ca^{2+} and Mg^{2+} supplemented with 2mM EDTA (Sigma-Aldrich, St. Louis, MO) and layered over a double discontinuous Ficoll-Percoll gradient (specific gravity 1.077 g/mL of Ficoll over 1.119 g/mL of Percoll; Sigma-Aldrich) in 15 mL conical centrifuge tubes, and centrifuged at 200g without brakes for 30 min at 4°C. The PBMC ring was collected at the Ficoll/supernatant interface and washed with PBS without Ca^{2+} and Mg^{2+} + 2mM EDTA to remove the contaminating thrombocytes. Red blood cells were eliminated using the Red Blood Cell Lysis Buffer (Roche Diagnostics GmbH, Mannheim, Germany). Finally, the PBMC were counted, their viability assessed with trypan blue exclusion, and resuspended at the desired concentration in complete medium (RPMI 1640 Medium + 25 mM HEPES + L-Glutamine, supplemented with 1% of Nonessential Amino Acid Solution 100X and 1% Penicillin Streptomycin Solution 100X and 1% FBS (Sigma-Aldrich)).

Chicken PBMC Stimulation With CP

Firstly, pectin esterified (55−70%) potassium salt from citrus fruit (Sigma-Aldrich) was prepared as previously described for chicken monocytes (Ávila et al., 2021) with some minor modifications. Briefly, only a working dilution of 0.5 mg/mL CP was prepared with the complete medium (1% FBS) freshly prepared for each experiment, and it was set as the working concentration for the stimulation of chicken PBMC. A total of 5×10^6 chicken PBMC (1.5 mL) were seeded in triplicates in Corning® tissue-culture treated culture 60 mm dishes (Corning Inc., Costar, Kennebunk, ME), with each set of triplicates corresponding to one of the 7 biological replicates (each from a different chicken blood pool). Cells were then incubated with 0.5 mg/mL of CP (500 μL) for 20 h at 41°C in a humified atmosphere with 5% CO_2. Complete medium (1% FBS) was then added to each dish to reach a final volume of 3 mL. These biological replicates were treated independently to account for biological variability.

Chicken PBMC Collection and Protein Extraction

After incubation, the cells' supernatant (3 mL), containing the cells in suspension (lymphocytes), was collected into 2 tubes of 1.5 mL. Cells were centrifuged at 500 × g for 7 min at 4°C to obtain the lymphocyte pellet. The lymphocyte pellet was washed twice with 500 μL sterile-PBS without Ca^{2+} and Mg^{2+} (room temperature) and again centrifuged twice at 500 x g for 7 min at 4°C to remove medium and FBS that could interfere with the proteomic analysis. In the meantime, 3 washes with 2 mL of sterile-PBS without Ca^{2+} and Mg^{2+} (room temperature) were performed in the 60 mm dishes to wash the adherent cells (monocytes) and remove dead cells and the rest

of the contaminant medium and FBS. When both the lymphocytes pellet and the adhered monocytes were washed, 500 μL of Igepal buffer (150 mM NaCl, 10 mM Tris-HCl pH 7.4, 1 mM EDTA and EGTA, 100 mM NaF, 4 mM $Na_4P_2O_7{\cdot}10\ H_2O$, 2 mM Na_3VO_4, 1% Triton X100, 0.5% IGEPAL CA-630 (Sigma-Aldrich), 1 tablet for 50 mL of the total volume of Protease Inhibitor Cocktail [Roche]) was added to the lymphocytes pellet. The cells were resuspended, then collected and added directly to the 60 mm wells containing the monocytes. The wells were then carefully mixed to ensure all surfaces were covered with Igepal buffer and incubated for 1h at 4°C with regular shaking to lyse the cells. After incubation, the cells were scraped using sterile Corning Cell scrapers (blade L 1.8 cm, handle L 25 cm; Corning Inc.), the cell lysate was collected in 1.5 mL tubes and sonicated for 10 min in an ultrasonic bath (Branson 2200, Danbury, CT) to complete the cells' lysis and homogenization. Finally, the tubes with the cell lysate were centrifuged for 10 min at 6000 x g at 4°C to remove the cell debris, and the supernatant containing the extracted proteins of all 3 technical replicates for each biological replicate was pooled in 1.5 mL tubes, aliquoted and stored at -80°C for further analyses.

Sample Preparation for Proteomic Analysis

Total protein concentration was first determined with the Pierce Bicinchoninic acid (**BCA**) protein assay kit (Thermo Fisher Scientific, Rockford, IL, USA), following the manufacturer's instructions. For peptide preparation, extracted proteins were digested and concentrated using the Filter Aided Sample Preparation (**FASP**) method, following the manufacturer's instructions with minor modifications. Briefly, fifty μg of protein lysate were put into Millipore 10 kDa MWCO filters, and 100 μl of Urea 8 M in 0.1 M Tris-HCl pH 8.5 were added for solubilization. The detergent and other contaminant components within the protein lysate were removed by repeated filtration by centrifugation. After discarding the flow-through, proteins were reduced with 100 μl DTT (10 mM) for 46 min and centrifuged at 14000 rpm for 10 min. Then, 200 μl of 25 mM iodoacetamide solution were added to the filters and incubated for 20 min at room temperature for protein alkylation. After performing several washes of the filters with Urea 8 M and 50 mM of ammonium bicarbonate, proteins were digested with 200 μl of 0.25 mg/mL trypsin (50:1 ratio of protein: enzyme) and mixed at 600 rpm in a thermomixer for 1 min. Filters were transferred to new collection tubes and incubated overnight in a wet chamber at 37°C. Finally, peptides were eluted by adding 200 μl of 50 mM of ammonium bicarbonate, and the filtrate was lyophilized in a SpeedVac and then resuspended in 100 μl of 1% formic acid.

Nano-LC-MS/MS Analysis

For each sample, 50μg of proteins were used according to the FASP preparation. The final volume was adjusted to 300 μL with a recovery solution (H_2O/ACN/TFA − 94.95/5/0.05). After passing through the ultrasonic bath (10 min), the supernatant was transferred to an HPLC vial before LC-MS/MS analysis. Peptide mixtures were analyzed by nano-LC-MS/MS (ThermoFisher Scientific) using an Ultimate 3000 system coupled to a QExactive HF-X mass spectrometer (MS) with a nanoelectrospray ion source. Five μL of hydrolyzate was first preconcentrated and desalted at a flow rate of 30 μl/mn on a C18 precolumn 5 cm length x 100 μm (Acclaim PepMap 100 C18, 5μm, 100A nanoViper) equilibrated with Trifluoroacetic Acid 0.05% in water. After 6 min, the concentration column was switched online with a nanodebit analytical C18 column (Acclaim PepMap 100 - 75 μm inner diameter × 25 cm length; C18 - 3 μm -100Å - SN 20106770) operating at 400 nL/min equilibrated with 96 % solvent A (99.9 % H2O, 0.1 % formic acid). The peptides were then separated according to their hydrophobicity thanks to a gradient of solvent B (99.9 % acetonitrile, 0.1 % formic acid) of 4 to 25% in 60 min. For MS analysis, eluted peptides were electrosprayed in positive-ion mode at 1.6 kV through a Nano electrospray ion source heated to 250°C. The mass spectrometer operated in data-dependent mode: the parent ion is selected in the orbitrap cell (FTMS) at a resolution of 60,000, and 18 MS/MS succeeds each MS analysis with analysis of the MS/MS fragments at a resolution of 15,000).

Processing of Raw Mass Spectrometry Data

At the end of the LC-MS/MS analysis, for raw data processing, a MS/MS ion search was carried out with Mascot v2.5.1 (http://www.matrixscience.com) against the chicken database (i.e., ref_Gallus gallus 210114-27,536 sequences). The following parameters were used during the request: precursor mass tolerance of 10 ppm and fragment mass tolerance of 0.02 Da, a maximum of 2 missed cleavage sites of trypsin, carbamidomethylation (**C**), oxidation (M) and deamidation (NQ) set as variable modifications. Protein identification was validated when at least 2 peptides originating from 1 protein showed statistically significant identity above Mascot scores with a False Discovery Rate of 1%. Ions score is -10 log(P), where P is the probability that an observed match is a random event. For the chicken proteome, the Mascot score was 31, with a false discovery rate (**FDR**) of 1%. The adjusted p-value was 0.02357. Finally, LC-Progenesis QI software (version 4.2, Nonlinear Dynamics, Newcastle upon Tyne, UK) was used for label-free protein quantification analysis with the same identification parameters described above with the phenotypic data among all matrices. All unique validated peptides of an identified protein were included, and the total cumulative abundance was calculated by summing the abundances of all

peptides allocated to the respective protein. LC-Progenesis analysis yielded 1503 unique quantifiable proteins, with at least 2 and 2 unique peptides.

Statistical Analyses

For all of the analyses, R version 4.2.2 was used.

Univariate analysis. To identify the differentially abundant proteins, a univariate statistical approach was performed on all 1503 quantified proteins, using an R package for proteomic analysis (available on GitHub with the DOI https://doi.org/10.5281/zenodo.2539329) as previously described (Bazile et al., 2019). Briefly, data normality distribution was assessed by the Shapiro-Wilk-Test. Then, a paired Student's t-test for normally distributed data and a paired Wilcoxon test for nondistributed data were applied to determine the p-value. Finally, the obtained p-values were corrected using different adjustment methods (e.g., Benjamini & Hochberg or FDR, Hochberg, and Bonferroni).

Multivariate analysis. As no differentially abundant proteins were obtained after performing the p-value corrections, an alternative supervised multilevel sparse variant partial least square discriminant analysis (sPLS-DA) was applied using the mixOmics package in R. The multilevel sPLS-DA enables the selection of the most predictive or discriminative proteins in the data of the 2 components (PC1 and PC2) to classify or cluster the samples between the 2 treatment groups (Lê Cao et al., 2011). With this supervised method and the mixOmics function plotLoadings() − Loadings Bar Plot, it was also possible to identify the discriminant proteins that presented higher abundances (median) in each treatment group. Thus, proteins with the highest abundance in the CP group also have a low abundance in the control groups and *vice versa*. We analyzed the importance of the ranked protein in discriminating between CP and control groups in component projection scores. However, only the proteins from the sPLS-DA component 1 that strongly correlated to one another (data given by the mixOmics function: plotVar() − Correlation Circle Plot) with the highest abundance in either the CP and control groups were used to perform further bioinformatic analyses (GO enrichment analyses).

Bioinformatic Analysis of Discriminant Proteins Selected by sPLS-DA

First, before performing the bioinformatic and functional annotation analyses, the accession numbers from all 1503 quantified proteins were converted into Gene ID using the UniProt retrieve/ID mapping online tool. The Gene ID of human orthologs of chicken proteins was assigned for undefined proteins. Second, only for the selected discriminant proteins a gene ontology (**GO**) enrichment analysis focused on the Biological processes (**BP**) was performed using ProteINSIDE online tool version 2.0 (available at https://umrh-bioinfo.clermont.inrae.fr/ProteINSIDE_2/index.php?page=upload.php), as previously described (Kaspric et al., 2015), and using *Gallus gallus* as reference specie. Only significant (FDR < 0.05) GO BP terms were considered enriched and were used for further interpretation and figure creation. The enriched GO BP terms were summarized, and their enrichments were expressed as -log10 (FDR) for visualization on horizontal bar graphs plotted using GraphPad Prism 9.1.2 for Mac OS X, GraphPad Software (San Diego, California). Selected discriminant proteins were also subjected to protein-protein interaction (**PPI**) analyses using the ProteINSIDE online tool version 2.0, as previously described (Kaspric et al., 2015), to identify the proteins that have been experimentally detected to interact with each other within the Human. The PPI databases used were IMEx, IntAct, and iRefIndex, which were chosen because they were updated in 2023. A network provided as a result was obtained for the 50 proteins CP related to the CP group. It was then filtered using the betweenness centrality values of 80 to 131 (high-degree nodes that mean shortest paths between nodes) algorithm (Kaspric et al., 2014), which was proven efficient in selecting key nodes/proteins within a pathway. The network obtained for the 137 proteins related to the control group or the inhibitory impact of the CP treatment was reduced by filtering using betweenness centrality values of 250 to 696. Finally, the average log fold-change (log FC) of the raw abundances of all the discriminant proteins identified with sPLS-DA from all 7 biological replicates was calculated and plotted using R version 3.6.3. In the plot, proteins with greater fold changes in their abundances showed bigger font sizes for better visualization.

RESULTS

The Proteome of Chicken PBMC and identification of the molecular signature of CP treatment

Hematoxylin eosin staining revealed that the PBMC population contained lymphocytes (72%), monocytes (9%), and heterophils (29%). 1503 proteins, with at least 2 unique peptides, were identified and quantified in chicken PBMC (Supplementary Table S1). A classical univariate statistical analysis (paired t-test or Wilcoxon test) did not detect any differentially abundant proteins between the CP and control groups after adjusting the *P*-value (FDR and Bonferroni). On the contrary, a multivariate sPLS-DA analysis applied to retrieve meaningful biological information and identify the molecular signature of CP treatment highlighted 373 discriminant proteins (approximately 25% of the overall total proteins identified) from both components (Supplementary Table S2), allowing for a good clustering between the CP and control groups (Figure 1). From the 373 discriminant proteins, only the 187 proteins from the sPLS-DA component 1 that strongly correlated together for each treatment group were selected to perform separate GO

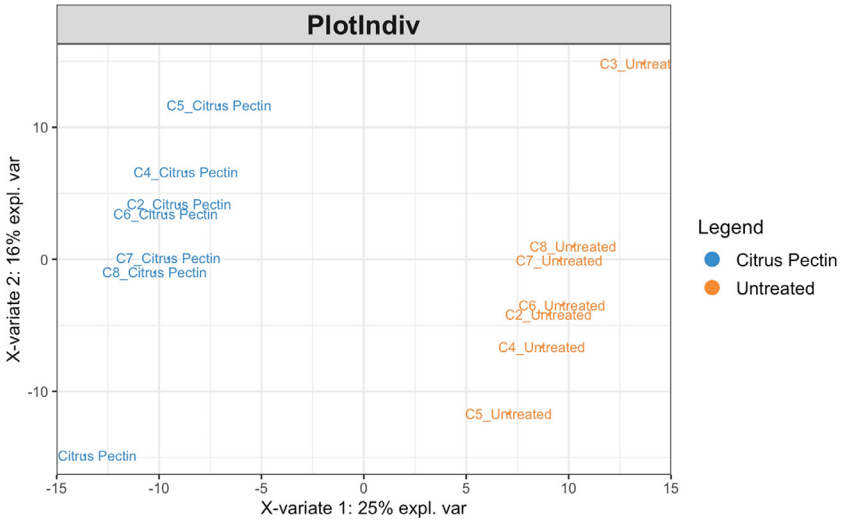

Figure 1. Sparse partial least squares discriminant analysis (sPLS-DA) for paired data individual plot. The individual plot shows the similarities and relationship (clustering) between samples of the citrus pectin (CP) (blue) and control (orange) treatment groups.

BP enrichment analyses. Of these proteins, 50 had the highest abundance in the CP group (and the lowest abundance in the control group), while 137 were identified with the highest abundance in the control group and thus as underabundant in the CP group (Supplementary Table S3).

GO Enrichment Analyses of Total Discriminant Proteins Identified by s-PLS-DA

A GO enrichment analysis identified the function of the 373 discriminant proteins. These 373 proteins were annotated by 121 enriched (FDR < 0.05) GO terms within the BP category. The main enriched BP were related to cellular amide metabolic process (GO:0043603), vesicle-mediated transport (GO:0016192), actin cytoskeleton organization (GO:0030036), peptide metabolic process (GO:0006518), organonitrogen compound biosynthesis (GO:1901566), actin filament organization (GO:0007015), translation (GO:0006412), cell migration (GO:0016477) and leukocyte chemotaxis regulation (GO:0002688) (Figure 2). From these enriched BP, the ones with the highest number of annotated proteins included: organonitrogen compound biosynthesis (49), vesicle-mediated transport (47), cellular amide metabolic processes (39) and cell migration (36) (Supplementary Table S4).

GO Enrichment Analyses of Discriminant Proteins Related to the CP Group

To further elucidate the differential effects of the CP and control treatments and the specific role of the discriminant proteins with the highest abundance in each group, separate GO enrichment analyses were carried out. The 50 proteins with the highest abundance in CP were annotated by 81 enriched (FDR < 0.05) GO terms within the

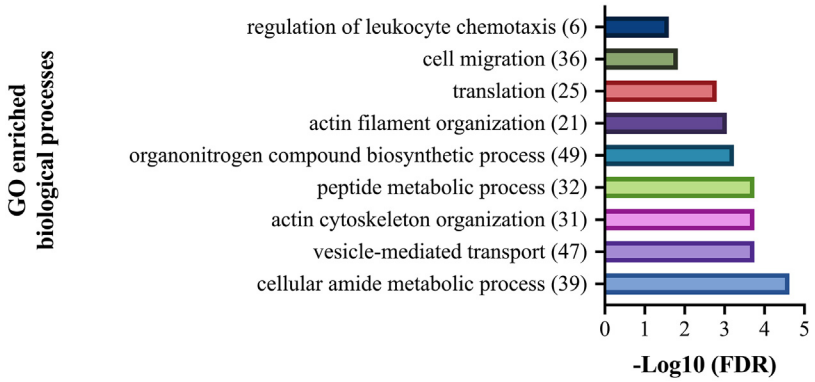

Figure 2. Global enriched ($P < 0.05$) Gene ontology (GO) terms within the biological processes (BP) category that has annotated all 373 discriminant proteins. GO terms enrichments are expressed as -log10 (FDR) for visualization on graphs. The number of proteins annotated by GO BP terms is shown in brackets.

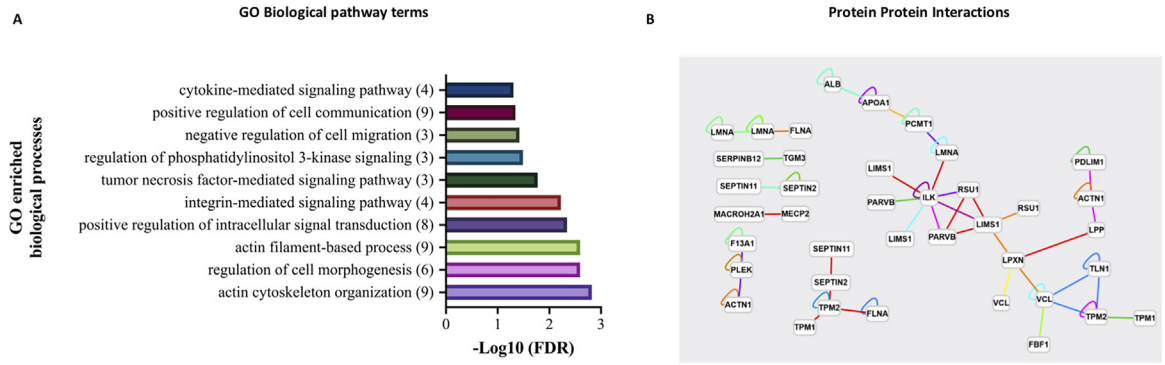

Figure 3. Enriched (P < 0.05) Gene ontology (GO) terms within the biological processes category that have annotated the 50 discriminant proteins with the highest abundance in the citrus pectin (CP) group. GO terms enrichments are expressed as -log10 (FDR) for visualization on graphs. (A) *The* GO Biological pathways terms. The number of proteins annotated by GO BP terms . The numbers of proteins annotaed by GO BP terms is shown in brackets. (B) Protein-Protein Interaction for the discriminant proteins with higher abundance in the citrus pectin (CP) group.

BP category. These proteins were mainly involved actin cytoskeleton organization (GO:0030036), regulation of cell morphogenesis (GO:0022604), actin filament-based process (GO:0030029), positive regulation of intracellular signal transduction (GO:1902533), integrin-mediated signaling pathway (GO:0007229), tumor necrosis factor-mediated signaling pathway (GO:0033209), regulation of phosphatidylinositol 3-kinase signaling (GO:0014066), negative regulation of cell migration (GO:0030336), positive regulation of cell communication (GO:0010647) and cytokine-mediated signaling pathway (GO:0019221). From these enriched BP, the ones with the highest number of annotated proteins were actin cytoskeleton, actin filament-based process and positive regulation of cell communication with 9 proteins, and positive regulation of intracellular transduction with 8 proteins (Figure 3A). APOA1 and SLC9A3R1 proteins were mainly annotated by almost all these enriched BP, and TLN1 on those related to the actin cytoskeleton and actin-filament organization and cell morphogenesis (Supplementary Table S5). The proteins related to the CP group were involved in 1 PPI major network and 6 additional small networks (Figure 3B). Within the major network, ILK, LPXN, and LIMS1 were the proteins with the shortest path with others, suggesting they are central in the pathway.

GO Enrichment Analyses of Discriminant Proteins Related to the Control Group

Among the 373 discriminant proteins that contributed to a good clustering between the 2 treatment groups, a higher number (137) was found to be more abundant in the control group. These proteins were annotated by 55 enriched (FDR < 0.05) BP GO terms related to the cellular amide metabolic process (GO:0043603), peptide metabolic process (GO:0006518), organonitrogen compound biosynthetic process (GO:1901566), translation (GO:0006412), catabolic process (GO:0009056), cellular homeostasis (GO:0019725), carbohydrate metabolic process (GO:0005975) and post-transcriptional regulation of gene expression (GO:0010608) (Figure 4A). The enriched BP with the highest number of annotated proteins were involved in different metabolic processes (> 20) and translation (16) (Supplementary Table S6). The proteins related to the control group were related to 1 PPI major network. By applying the betweenness centrality filter

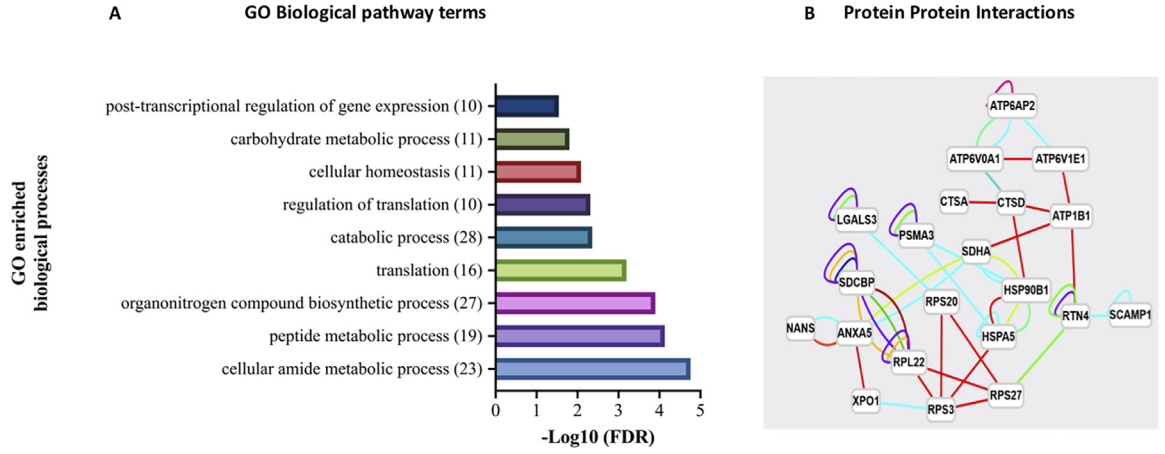

Figure 4. Enriched ($P < 0.05$) Gene ontology (GO) terms within the biological processes category that have annotated the 137 discriminant proteins with the highest abundance in the control group (no CP). (A) GO terms enrichments are expressed as -log10 (FDR) for visualization on graphs. The number of proteins annotated by GO BP terms is shown in brackets. (B) Protein-Protein Interaction for the discriminant proteins with higher abundance in the control group (no CP).

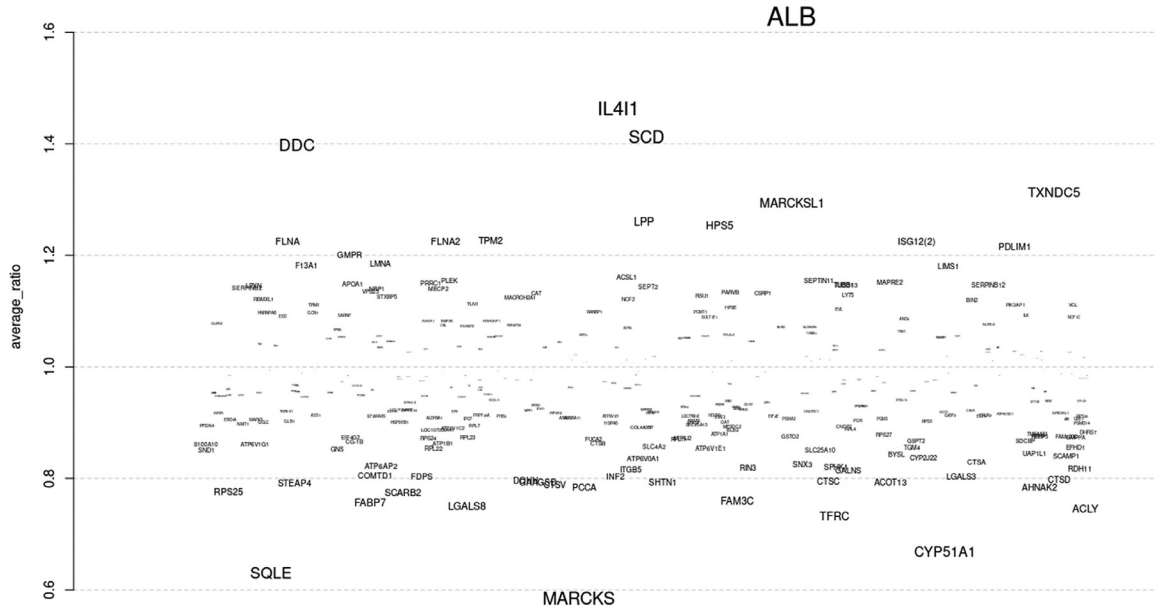

Figure 5. Figure 2 Average fold-change of protein raw abundances of the discriminant proteins (DP) selected by sPLS-DA. The y-axis shows the average log fold-change (average ratio) of the raw abundances from all the different biological replicates (samples) after Citrus Pectin treatment, with respect to the control group.

(Figure 4B), we identified SDHA, HSP90B1, HSPA9, RPS3, and RTN4 as the proteins with the shortest path with others, suggesting they are central in the pathway.

Average Fold-Change of the Abundances of the Discriminant Proteins Identified With sPLS-DA

Lastly, to have a more straightforward overview of the changes in abundances of all the 373 discriminant proteins between the CP and control groups, we calculated the average fold-change of the raw abundances of the proteins from the cells treated with CP (Figure 5). The protein with the most significant change in abundance (FC > 1.6) between the CP and control was ALB. Other proteins with higher abundances in the CP group included SCD and IL4I1 (FC ≥1.4), and FLNA, TPM2, ISG12(2), PDLIM1, LPP, HPS5, TXNDC5 and MARCKSL1 (FC > 1.2). On the other hand, proteins such as MARCKS, LGALS8, LGALS3, SQLE, CYP51A1, FABP7, FAM3C, TFRC, and AHNAK2 showed the lowest abundance in the CP group (FC ≤ 0.8).

DISCUSSION

The present study describes the proteome of mononuclear cells after stimulation with CP. In previous studies, CP was shown to inhibit monocytes' chemotaxis and phagocytosis (Ávila et al., 2021). The present main findings were that CP induced the downregulation of Biological Processes related to actin cytoskeleton organization, cell migration, intracellular signal transduction, and cell communication: we, therefore, provided a molecular background to the immunomodulatory and anti-inflammatory activity previously demonstrated (Ávila et al., 2021).

Global Biological Processes Enriched by the Discriminant Proteins Selected by *sPLS-DA*

In the first part of the study, a sPLS-DA model was applied to identify the molecular signature of CP treatment, allowing the selection of the most discriminative features or proteins in the data to classify the samples (Lê Cao et al., 2011), including 373 discriminant proteins, and enabling to discriminate the samples between the CP and control groups adequately. Proteins with a mean abundance of the highest (50 proteins) and lowest (137 proteins) in the CP group were mined. To have a global idea of the function of these discriminant proteins, a GO enrichment analysis was carried out, revealing that these proteins were involved in very general BP processes related to metabolisms, like cellular amide and peptide metabolic process, organonitrogen compound biosynthetic process, and translation, and enriching for other more specific cell shape- or immune-related processes, such as the actin cytoskeleton and actin filament organization, vesicle-mediated transport, cell migration, and regulation of leukocyte chemotaxis.

Biological Processes Enriched by Discriminant Proteins With the Highest Abundance After CP Treatment

In the second part of the study, separate GO enrichment analyses further elucidated the specific function of the discriminant proteins identified for the CP and control group, using the proteins with the highest abundance in each group. The 50

discriminant proteins with the highest abundance in the CP group were mainly related to actin cytoskeleton organization, cell morphogenesis regulation, positive regulation of intracellular signal transduction, positive regulation of cell communication, and negative regulation of cell migration.

The ability of cells to rapidly change their morphology in response to activation is an important feature of immune cells and their effector functions. The actin cytoskeleton plays a critical role in providing the cells with the mechanical structure to support their changes in shape and membrane (Rivero et al., 1996), being involved, as such, in chemotaxis and phagocytosis (May and Machesky, 2001; Affolter and Weijer, 2005).

Talin-1 (TLN1) and Na(+)/H(+) exchange regulatory cofactor (NHERF1/SLC9A3R1) were 2 of the proteins annotated for the actin cytoskeleton organization and actin filament-based process GO BP terms. TLN1 is involved in phagocytosis and phagosome formation by providing a physical link between the actin cytoskeleton and integrin receptors (Lim et al., 2007)(Torres-Gomez et al., 2020). SLC9A3R1 is a scaffold protein that stabilizes protein complexes at the plasma membrane by connecting signaling pathways and structural proteins to the actin cytoskeleton and is related to the negative regulation of cell migration (Bretscher et al., 2000). The findings are consistent with previous reports on lung cancer cells, where overexpression of the SLC9A3R1 protein inhibited the cells' migration (Yang et al., 2017). This result is remarkable, as we previously demonstrated that CP inhibited chicken monocyte chemotaxis *in vitro* (Ávila et al., 2021), as described for other pectins, like ginseng (Fan et al., 2018).

Enrichment of immune and inflammation-related pathways, like tumor necrosis, regulation of phosphatidylinositol 3-kinase, and cytokine-mediated signaling pathways, was observed in the CP group, further suggesting immunomodulatory activities of CP. Apolipoprotein A-I (**APOA1**) was one of the proteins annotated in almost all the enriched GO BP terms, including the tumor necrosis signaling and cytokine-mediated signaling pathways. APOA1 inhibits macrophage chemotaxis and monocyte recruitment by modulating the reorganization of the actin component of the cytoskeleton (Iqbal et al., 2016). The current results are consistent with a previous study on mice fed with pectin oligosaccharides that increased APOA1 levels in plasma (Zhu et al., 2017). Our proteomics findings showed that the immunomodulatory activity of CP toward PBMC is related to changes in their actin cytoskeleton organization and signal transduction pathways, often critical for the regulation of phagocytosis and cell migration, as well as cell communication and inflammation.

In contrast with the enriched BP found in the CP group, the enriched BP in the control group were very general GO terms related mainly to different metabolic processes, translation, cellular homeostasis, and post-transcriptional regulation of gene expression.

Discriminant Proteins With Greater Changes in Abundance After CP Treatment

To further elucidate the effects of CP on chicken PBMC proteome and determine its molecular signature, we focused on identifying essential proteins mostly changed in their raw abundances when treated with CP, considering their fold-change, and that could be involved in the most enriched BP detected with the GO analysis.

The protein with the highest abundance after CP treatment was albumin (**ALB**), the most abundant circulating protein in plasma, whose main activity is to transport fatty acids, cholesterol, metals, and other components (Park et al., 2014). Albumin also works as a significant antioxidant protein by trapping free radicals, a negative acute-phase protein, a negative regulator of apoptosis in endothelial cells: we may then speculate that, by increasing ALB abundance, CP might exert protective effects in chicken PBMC against oxidative stress and apoptosis (Zoellner et al., 1996; Roche et al., 2008; Marques et al., 2017). Other proteins with the highest abundances in the CP group and involved with immune response included serum amyloid A protein (HPS5), an acute-phase response protein in chicken (Marques et al., 2017), L-amino-acid oxidase (IL4I1), a negative regulator of T cell activation/proliferation and adaptive immunity (Castellano and Molinier-Frenkel, 2017), the putative ISG12(2) protein and the uncharacterized protein TXNDC5, both related with negative regulation of apoptosis processes (Horna-Terrón et al., 2014; Qi et al., 2015). Remarkably, the analysis of the discriminant proteins with greater changes in abundance after CP treatment also confirms a rearrangement of the cytoskeleton as shown by the upregulation in the CP group of Myristoylated alanine-rich C kinase substrate-like 1 (**MARCKSL1**) protein. MARCKSL1 is a membrane-bound protein part of the MARCKS family with known actin-binding functions that regulate actin cytoskeleton homeostasis and coordinate other membrane-cytoskeletal signaling events such as cell migration and phagocytosis (Kim et al., 2016). MARCKSL1 is highly expressed in macrophages and is involved in macrophage transmigration (Chun et al., 2009). These results are consistent with the suppression of chicken monocytes' chemotaxis observed in our previous *in vitro* study (Ávila et al., 2021).

Other proteins highly abundant in the CP group include Filamin-A (**FLNA**), tropomyosin beta chain (**TPM2**), the uncharacterized protein (**PDLIM1**), and lipoma-preferred partner homolog (**LPP**): all these 4 proteins have also been associated with actin cytoskeleton organization and stabilization (Gunning et al., 2008; Ono et al., 2015; Welter et al., 2020), cell migration (Savinko et al., 2018), maintaining cell shape and cell adhesion (Petit et al., 2000; Ngan et al., 2018). The CP group also included the fatty acid-desaturase domain-containing (SCD) protein involved with fatty acid biosynthesis related to humoral immune responses (Zhou et al., 2021).

On the contrary, proteins such as MARCKS, LGALS3, and LGALS8 were less abundant in the CP group. Specifically, MARCKS has been shown to promote murine macrophage migration (Green et al., 2012), phagocytosis (Carballo et al., 1999), and proinflammatory cytokines production (Lee et al., 2015), confirming its involvement in modulating inflammation.

Some proteins were also less abundant in the CP group. Galectin-3 (LGALS3) and galectin-8 (LGALS8) are ubiquitous carbohydrate-binding proteins (Brinchmann et al., 2018) that participate in several cellular processes, such as inflammation, immune responses, cell migration, autophagy, and cell signaling. In chickens, 5 members have been identified (Kaltner et al., 2011): LGALS3 and LGALS. LGALS3 is highly expressed in monocytes and macrophages and is a potent regulator of cell-extracellular matrix (**ECM**) and cell-cell interactions, migration, and phagocytosis (Lu et al., 2017). The decreased abundance of LGALS3 in the CP group is also remarkable, as mouse LGALS3 was downregulated by modified citrus pectin (**MCP**)—a derivative of citrus pectin (Kolatsi-Joannou et al., 2011). MCP also directly inhibits LGALS3, decreasing the adhesion of monocytes and macrophages (Lu et al., 2017). LGALS8 is involved in cytoskeleton reorganization processes, cell adhesion, and cell migration, as well as in autophagy and cytokines and chemokines expression (Gentilini et al., 2017; Johannes et al., 2018). Finally, we also identified proteins involved in the positive regulation of T and B cell proliferation (TFRC) (Ned et al., 2003) and human mononuclear cell migration (AHNAK2) (Zheng et al., 2021), further supporting the CP immune-modulatory function.

CONCLUSIONS

In conclusion, the findings of this proteomics study provide a molecular background to previously reported *in vitro* immunomodulatory activity of CP toward PBMC by changing the abundance of proteins involved in actin cytoskeleton organization and cell migration. These findings confirm the suppressive effects observed in our *in vitro* study on chicken monocytes' phagocytosis and chemotaxis and report novel information on the immunomodulatory activity of CP on chicken PBMC. By elucidating the molecular mechanisms underlying such immunomodulatory effects, we might better understand CP's practical biological significance *in vivo* and how to include it as a dietary fiber in novel nutrition strategies to modulate the animals' immune and health status. Moreover, this study demonstrates the suitability of the supervised multivariate statistical analysis sPLS-DA to retrieve meaningful functional information from complex proteomics data, converting it into a noteworthy option for analyzing data from other OMIC technologies. Further functional annotation analyses such as molecular pathway enrichment, protein-protein interaction analyses, and integration of proteomics data with other OMIC technologies are required to deepen the overall impact of CP on chicken immunity knowledge.

The description of the molecular basis of the immunomodulatory activity of CP will provide the nutritionists with important feedback: while the use of CP has been regarded as a valuable feed additive in chicken feeding, and indeed an anti-inflammatory activity is also considered beneficial, to avoid the excessive inflammatory reaction that can do more harm than good if uncontrolled, still an anti-inflammatory activity, if not adequately balanced, may weaken the immune system. Therefore, the results of this molecular study will also raise awareness about the excessive use of anti-inflammatory drugs. Further studies are required to assess the in vivo impact of CP additive in diets during diseases.

ACKNOWLEDGMENTS

This work is part of the PhD thesis of Gabriela Avila Morales (https://air.unimi.it/handle/2434/952952?mode=full). The authors acknowledge A. Delavaud (INRAE, Herbivore Research Unit) for his technical assistance in protein extraction, quantification, and concentration for mass spectrometry analyses, and also Arnaud Cougoul, Jeremy Tournayre and Céline Boby (INRAE, Herbivore Research Unit) for their assistance in the statistical and bioinformatic analyses, respectively. This study was supported by the European Union's Horizon 2020 research and innovation programme H2020-MSCA- ITN-2017- EJD: Marie Skłodowska-Curie Innovative Training Networks (European Joint Doctorate) [Grant agreement n°: 765423, 2017] – MANNA.

Ethics statement: All applicable international, national, and/or institutional guidelines for the care and use of animals were followed. The procedures for the blood collection were carried out during routine slaughtering procedures.

DISCLOSURES

None of the authors of this paper has a financial or personal relationship with other people or organizations that could inappropriately influence or bias the paper's content.

SUPPLEMENTARY MATERIALS

Supplementary material associated with this article can be found, in the online version, at doi:10.1016/j.psj.2024.104293.

REFERENCES

Affolter, M., and C. J. Weijer. 2005. Signaling to cytoskeletal dynamics during chemotaxis. Dev. Cell 9:19–34.

Ahmad, F., A. Sultan, S. Khan, M. Ali, I. Ali, H. Abdullah, G. M. Suliman, and A. A. Swelum. 2024. Effect of citrus peeling (Citrus sinensis) on production performance, humoral immunity, nutrients, and energy utilization of broiler quails. Poult. Sci.

103:103207. Available at http://www.ncbi.nlm.nih.gov/pubmed/37931398.

Almeida, A. M., S. A. Ali, F. Ceciliani, P. D. Eckersall, L. E. Hernández-Castellano, R. Han, J. J. Hodnik, S. Jaswal, J. D. Lippolis, M. McLaughlin, I. Miller, A. K. Mohanty, V. Mrljak, J. E. Nally, P. Nanni, J. E. Plowman, M. D. Poleti, D. M. Ribeiro, P. Rodrigues, B. Roschitzki, R. Schlapbach, J. Starič, Y. Yang, and M. Zachut. 2021. Domestic animal proteomics in the 21st century: A global retrospective and viewpoint analysis. J. Proteomics 241:104220. Available at https://linkinghub.elsevier.com/retrieve/pii/S1874391921001196.

Ávila, G., D. De Leonardis, G. Grilli, C. Lecchi, and F. Ceciliani. 2021. Anti-inflammatory activity of citrus pectin on chicken monocytes' immune response. Vet. Immunol. Immunopathol. 237:110269.

Bazile, J., B. Picard, C. Chambon, A. Valais, and M. Bonnet. 2019. Pathways and biomarkers of marbling and carcass fat deposition in bovine revealed by a combination of gel-based and gel-free proteomic analyses. Meat Sci 156:146–155.

Beukema, M., M. M. Faas, and P. de Vos. 2020. The effects of different dietary fiber pectin structures on the gastrointestinal immune barrier: impact via gut microbiota and direct effects on immune cells. Exp. Mol. Med. 52:1364–1376.

Bretscher, A., D. Chambers, R. Nguyen, and D. Reczek. 2000. ERM-Merlin and EBP50 Protein Families in Plasma Membrane Organization and Function. Annu. Rev. Cell Dev. Biol. 16:113–143.

Brinchmann, M. F., D. M. Patel, and M. H. Iversen. 2018. The role of galectins as modulators of metabolism and inflammation.Mediators Inflamm 2018:9186940.

Carballo, E., D. M. Pitterle, D. J. Stumpo, R. T. Sperling, and P. J. Blackshear. 1999. Phagocytic and macropinocytic activity in MARCKS-deficient macrophages and fibroblasts. Am. J. Physiol. Physiol. 277:C163–C173.

Castellano, F., and V. Molinier-Frenkel. 2017. An overview of l-Amino acid oxidase functions from bacteria to mammals: Focus on the immunoregulatory phenylalanine oxidase IL4I1. Molecules 22:2151.

Chun, K.-R., E. M. Bae, J.-K. Kim, K. Suk, and W.-H. Lee. 2009. Suppression of the lipopolysaccharide-induced expression of MARCKS-related protein (MRP) affects transmigration in activated RAW264.7 cells. Cell. Immunol. 256:92–98.

de Paula Menezes Barbosa, P., A. Roggia Ruviaro, I. Mateus Martins, J. Alves Macedo, G. LaPointe, and G. Alves Macedo. 2020. Effect of enzymatic treatment of citrus by-products on bacterial growth, adhesion and cytokine production by Caco-2 cells. Food Funct 11:8996–9009. Available at http://www.ncbi.nlm.nih.gov/pubmed/33007056.

Deeg, C. A., R. L. Degroote, I. M. Giese, S. Hirmer, B. Amann, M. Weigand, C. Wiedemann, and S. M. Hauck. 2020. CD11d is a novel antigen on chicken leukocytes. J. Proteomics 225:103876. Available at http://www.ncbi.nlm.nih.gov/pubmed/32534212.

Deng, X., Y. Cong, R. Yin, G. Yang, C. Ding, S. Yu, X. Liu, C. Wang, and Z. Ding. 2014. Proteomic analysis of chicken peripheral blood mononuclear cells after infection by Newcastle disease virus. J. Vet. Sci 15:511–517.

Fan, Y., L. Sun, S. Yang, C. He, G. Tai, and Y. Zhou. 2018. The roles and mechanisms of homogalacturonan and rhamnogalacturonan I pectins on the inhibition of cell migration. Int. J. Biol. Macromol. 106:207–217.

Gentilini, L. D., F. M. Jaworski, C. Tiraboschi, I. G. Pérez, M. L. Kotler, A. Chauchereau, D. J. Laderach, and D. Compagno. 2017. Stable and high expression of Galectin-8 tightly controls metastatic progression of prostate cancer. Oncotarget 8:44654–44668.

Green, T. D., J. Park, Q. Yin, S. Fang, A. L. Crews, S. L. Jones, and K. B. Adler. 2012. Directed migration of mouse macrophages in vitro involves myristoylated alanine-rich C-kinase substrate (MARCKS) protein. J. Leukoc. Biol. 92:633–639.

Gunning, P., G. O'neill, and E. Hardeman. 2008. Tropomyosin-based regulation of the actin cytoskeleton in time and space. Physiol. Rev. 88:1–35.

Horna-Terrón, E., A. Pradilla-Dieste, C. Sánchez-de-Diego, and J. Osada. 2014. TXNDC5, a newly discovered disulfide isomerase with a key role in cell physiology and pathology. Int. J. Mol. Sci. 15:23501–23518.

Iqbal, A. J., T. J. Barrett, L. Taylor, E. McNeill, A. Manmadhan, C. Recio, A. Carmineri, M. H. Brodermann, G. E. White, D. Cooper, J. A. DiDonato, M. Zamanian-Daryoush, S. L. Hazen, K. M. Channon, D. R. Greaves, and E. A. Fisher. 2016. Acute exposure to apolipoprotein A1 inhibits macrophage chemotaxis in vitro and monocyte recruitment in vivo (CK Glass, Ed.). Elife 5:e15190.

Johannes, L., R. Jacob, and H. Leffler. 2018. Galectins at a glance. J. Cell Sci. 131:jcs208884.

Kaltner, H., D. Kübler, L. López-Merino, M. Lohr, J. C. Manning, M. Lensch, J. Seidler, W. D. Lehmann, S. André, and D. Solís. 2011. Toward comprehensive analysis of the galectin network in chicken: Unique diversity of galectin-3 and comparison of its localization profile in organs of adult animals to the other four members of this lectin family. Anat. Rec. Adv. Integr. Anat. Evol. Biol. 294:427–444.

Kaspric, N., B. Picard, M. Reichstadt, J. Tournayre, and M. Bonnet. 2014. Protein function easily investigated by genomics data mining using the ProteINSIDE web service.

Kaspric, N., B. Picard, M. Reichstadt, J. Tournayre, and M. Bonnet. 2015. ProteINSIDE to easily investigate proteomics data from ruminants: application to mine proteome of adipose and muscle tissues in bovine foetuses. PLoS One 10:e0128086.

Kim, B.-R., S.-H. Lee, M.-S. Park, S.-H. Seo, Y.-M. Park, Y.-J. Kwon, and S.-B. Rho. 2016. MARCKSL1 exhibits anti-angiogenic effects through suppression of VEGFR-2-dependent Akt/PDK-1/mTOR phosphorylation. Oncol. Rep 35:1041–1048.

Kolatsi-Joannou, M., K. L. Price, P. J. Winyard, and D. A. Long. 2011. Modified citrus pectin reduces Galectin-3 expression and disease severity in experimental acute kidney injury. PLoS One 6:e18683.

Korte, J., T. Fröhlich, M. Kohn, B. Kaspers, G. J. Arnold, and S. Härtle. 2013. 2D DIGE analysis of the bursa of Fabricius reveals characteristic proteome profiles for different stages of chicken B-cell development. Proteomics 13:119–133. Available at http://www.ncbi.nlm.nih.gov/pubmed/23135993.

Langhout, D. J., and J. B. Schutte. 1996. Nutritional implications of pectins in chicks in relation to esterification and origin of pectins. Poult. Sci. 75:1236–1242.

Lê Cao, K.-A., S. Boitard, and P. Besse. 2011. Sparse PLS discriminant analysis: biologically relevant feature selection and graphical displays for multiclass problems. BMC Bioinformatics 12:253.

Leclere, L., P. Van Cutsem, and C. Michiels. 2013. Anti-cancer activities of pH- or heat-modified pectin. Front. Pharmacol. 4:128.

Lee, S.-M., K. Suk, and W.-H. Lee. 2015. Myristoylated alanine-rich C kinase substrate (MARCKS) regulates the expression of proinflammatory cytokines in macrophages through activation of p38/JNK MAPK and NF-κB. Cell. Immunol. 296:115–121.

Lim, J., A. Wiedemann, G. Tzircotis, S. J. Monkley, D. R. Critchley, and E. Caron. 2007. An essential role for talin during alpha(M) beta(2)-mediated phagocytosis. Mol. Biol. Cell 18:976–985.

Lu, Y., M. Zhang, P. Zhao, M. Jia, B. Liu, Q. Jia, J. Guo, L. Dou, and J. Li. 2017. Modified citrus pectin inhibits galectin-3 function to reduce atherosclerotic lesions in apoE-deficient mice. Mol. Med. Rep 16:647–653.

Marques, A. T., L. Nordio, C. Lecchi, G. Grilli, C. Giudice, and F. Ceciliani. 2017. Widespread extrahepatic expression of acute-phase proteins in healthy chicken (Gallus gallus) tissues. Vet. Immunol. Immunopathol. 190:10–17. Available at https://linkinghub.elsevier.com/retrieve/pii/S0165242717300405.

May, R. C., and L. M. Machesky. 2001. Phagocytosis and the actin cytoskeleton. J. Cell Sci. 114:1061–1077.

Ned, R. M., W. Swat, and N. C. Andrews. 2003. Transferrin receptor 1 is differentially required in lymphocyte development. Blood 102:3711–3718.

Ngan, E., A. Kiepas, C. M. Brown, and P. M. Siegel. 2018. Emerging roles for LPP in metastatic cancer progression. J. Cell Commun. Signal. 12:143–156.

Ono, R., T. Kaisho, and T. Tanaka. 2015. PDLIM1 inhibits NF-κB-mediated inflammatory signaling by sequestering the p65 subunit of NF-κB in the cytoplasm. Sci. Rep. 5:18327.

Park, K. T., C.-H. Yun, C.-S. Bae, and T. Ahn. 2014. Decreased level of albumin in peripheral blood mononuclear cells of streptozotocin-induced diabetic rats. J. Vet. Med. Sci. 76:1087–1092.

Petit, M. M. R., J. Fradelizi, R. M. Golsteyn, T. A. Y. Ayoubi, B. Menichi, D. Louvard, W. J. M. Van de Ven, and E. Friederich. 2000. LPP, an Actin Cytoskeleton Protein Related to Zyxin, Harbors a Nuclear Export Signal and Transcriptional Activation Capacity. Mol. Biol. Cell 11:117–129.

Pourhossein, Z., A. A. A. Qotbi, A. Seidavi, V. Laudadio, G. Centoducati, and V. Tufarelli. 2015. Effect of different levels of dietary sweet orange (Citrus sinensis) peel extract on humoral immune system responses in broiler chickens. Anim. Sci. J. 86:105–110. Available at http://www.ncbi.nlm.nih.gov/pubmed/24990585.

Qi, Y., Y. Li, Y. Zhang, L. Zhang, Z. Wang, X. Zhang, L. Gui, and J. Huang. 2015. IFI6 inhibits apoptosis via mitochondrial-dependent pathway in dengue Virus 2 infected vascular endothelial cells. PLoS One 10:e0132743.

Ridley, B. L., M. A. O'Neill, and D. Mohnen. 2001. Pectins: structure, biosynthesis, and oligogalacturonide-related signaling. Phytochemistry 57:929–967.

Rivero, F., B. Koppel, B. Peracino, S. Bozzaro, F. Siegert, C. J. Weijer, M. Schleicher, R. Albrecht, and A. A. Noegel. 1996. The role of the cortical cytoskeleton: F-actin crosslinking proteins protect against osmotic stress, ensure cell size, cell shape and motility, and contribute to phagocytosis and development. J. Cell Sci. 109:2679–2691.

Roche, M., P. Rondeau, N. R. Singh, E. Tarnus, and E. Bourdon. 2008. The antioxidant properties of serum albumin. FEBS Lett 582:1783–1787.

Sahasrabudhe, N. M., M. Beukema, L. Tian, B. Troost, J. Scholte, E. Bruininx, G. Bruggeman, M. van den Berg, A. Scheurink, H. A. Schols, M. M. Faas, and P. de Vos. 2018. Dietary fiber pectin directly blocks toll-like receptor 2-1 and prevents doxorubicin-induced ileitis. Front. Immunol. 9:1–19.

Salman, H., M. Bergman, M. Djaldetti, J. Orlin, and H. Bessler. 2008. Citrus pectin affects cytokine production by human peripheral blood mononuclear cells. Biomed. Pharmacother. 62:579–582.

Savinko, T., C. Guenther, L. M. Uotila, M. Llort Asens, S. Yao, S. Tojkander, and S. C. Fagerholm. 2018. Filamin A is required for optimal T cell integrin-mediated force transmission, flow adhesion, and T Cell trafficking. J. Immunol. 200:3109.

Sekelova, Z., O. Polansky, H. Stepanova, R. Fedr, M. Faldynova, I. Rychlik, and L. Vlasatikova. 2017. Different roles of CD4, CD8 and $\gamma\delta$ T-lymphocytes in naive and vaccinated chickens during Salmonella Enteritidis infection. Proteomics 17:1–9.

Silva, V. K., V. de Souza Morita, and I. C. Boleli. 2013. Effect of pectin extracted from citrus pulp on digesta characteristics and nutrient digestibility in broilers chickens. Rev. Bras. Zootec. 42:575–583.

Sundaram, T. S., C. Giromini, R. Rebucci, J. Pistl, M. Bhide, and A. Baldi. 2022. Role of omega-3 polyunsaturated fatty acids, citrus pectin, and milk-derived exosomes on intestinal barrier integrity and immunity in animals. J. Anim. Sci. Biotechnol. 13:40. Available at http://www.ncbi.nlm.nih.gov/pubmed/35399093.

Torres-Gomez, A., C. Cabañas, and E. M. Lafuente. 2020. Phagocytic integrins: Activation and signaling. Front. Immunol. 11:738.

Welter, H., C. Herrmann, T. Fröhlich, F. Flenkenthaler, K. Eubler, H. Schorle, D. Nettersheim, A. Mayerhofer, and A. Müller-Taubenberger. 2020. Filamin A orchestrates cytoskeletal structure, cell migration and stem cell characteristics in human seminoma TCam-2 cells. Cells 9:2563.

Wils-Plotz, E. L., M. C. Jenkins, and R. N. Dilger. 2013. Modulation of the intestinal environment, innate immune response, and barrier function by dietary threonine and purified fiber during a coccidiosis challenge in broiler chicks. Poult. Sci. 92:735–745. Available at http://www.ncbi.nlm.nih.gov/pubmed/23436524.

Yang, F., Y. Gu, Z. Zhao, J. Huang, J. Weng, and S. Cheng. 2017. NHERF1 suppresses lung cancer cell migration by regulation of epithelial−mesenchymal transition. Anticancer Res 37:4405.

Zheng, L., S. Li, X. Zheng, R. Guo, and W. Qu. 2021. AHNAK2 is a novel prognostic marker and correlates with immune infiltration in papillary thyroid cancer: Evidence from integrated analysis. Int. Immunopharmacol. 90:107185.

Zhou, X., X. Zhu, and H. Zeng. 2021. Fatty acid metabolism in adaptive immunity. FEBS J 584–599.

Zhu, R.-G., Y.-D. Sun, Y.-T. Hou, J.-G. Fan, G. Chen, and T.-P. Li. 2017. Pectin penta-oligogalacturonide reduces cholesterol accumulation by promoting bile acid biosynthesis and excretion in high-cholesterol-fed mice. Chem. Biol. Interact. 272:153–159.

Zoellner, H., M. Hofler, R. Beckmann, P. Hufnagl, E. Vanyek, E. Bielek, J. Wojta, A. Fabry, S. Lockie, and B. R. Binder. 1996. Serum albumin is a specific inhibitor of apoptosis in human endothelial cells. J. Cell Sci. 109:2571–2580.